Chapter 4

System Identification and Controller Design

This chapter presents an optimal design for the tracking system with a PID compensator. First the transfer function model is obtained through frequency domain system identification. Model nonlinearities as well as model variations are treated as model uncertainties, while the performance index is augmented into system as a fictitious uncertainty. The stability and robust performance are sought by PID optimization on the tracking system. The simulation results show the optimal parameters of PID compensator in tracking system.

4.1 System Identification [22-24]

System identification is the process of developing or improving a mathematical representation of a physical system using experimental data. The mission of the system identification community for engineering systems is to provide effective and accurate analytical tools which include the underlying methodologies, computational procedures and their implementation. The development of good analytical tools demands a mathematical understanding of the problem to be solved and an appreciation for the numerical precision required when handling a large amount of data. This chapter described the frequency domain identification with MATLAB and Bode-plot as applied to the tracking system.

4.1.1 Frequency Domain Identification

The goal of the frequency domain identification is to find a transfer function whose bode-plot can approximate the measured frequency response. The normalized error index is defined as Eq. (4-1).

$$e^2 = \sum_{w=w_0}^{w_1} \left| \frac{\hat{G}(jw) - G_m(jw)}{\hat{G}(jw)} \right|^2, \qquad (4\text{-}1)$$

where $?_0$ and $?_1$ stand for the starting and terminal frequencies in the measurement, respectively.

Gm (j?) is the measured frequency response, and $\hat{G}$(j?) is the estimated transfer function. Normalized error rather than absolute error is minimized to obtain a better match at high frequencies. It is assumed that the estimated transfer function takes the from as Eq. (4-2),

$$\hat{G}(s) = \frac{\hat{b}_m s^m + \hat{b}_{m-1} s^{m-1} + ... + \hat{b}_1 s + \hat{b}_0}{s^n + \hat{a}_{n-1} s^{n-1} + ... + \hat{a}_1 s + \hat{a}_0}, \qquad (4\text{-}2)$$

where $\hat{a}_i$ and $\hat{b}_i$ are the coefficients of the numerator and denominator polynomials, respectively.

$$\frac{\hat{G}(jw) - G_m(jw)}{\hat{G}(jw)} = \frac{\hat{b}_m(jw)^m + \hat{b}_{m-1}(jw)^{m-1} + ... + \hat{b}_1(jw) + \hat{b}_0 - Gm(jw)[(jw)^n + \hat{a}_{n-1}(jw)^{n-1} + ... + \hat{a}_1(jw) + \hat{a}_0]}{\hat{b}_m(jw)^m + \hat{b}_{m-1}(jw)^{m-1} + ... + \hat{b}_1(jw) + \hat{b}_0}$$

(4-3)

By substituting s=j? into Eq. (4-2), the error index in Eq.(4-1) is expressed in Eq.(4-3) below, and minimized by a two-step Least Squares Estimation (LSE). In the first step, the numerator is minimized to get a rough estimation of the coefficients $\hat{a}_i$

and $\hat{b}_j$, i=1,2…n, j=1,2…m. Next, the coefficients $\hat{b}_i$ are substituted into the denominator to minimize e^2. The second step is repeated till the new parameters are close enough to the results obtained during the previous iteration.

The standard form of a LSE problem is given by

$$\mathbf{Y=XH + w} \tag{4-4}$$

Where **Y** is the output vector corrupted by white noise **w**, **X** is input matrix and **H** is the parameter vector. The identification procedure is as follows:

1. Compute the model parameters by using

$$\hat{\mathbf{H}} = (\mathbf{X}\mathbf{X}^{\mathbf{T}})^{-1}\mathbf{X}^{\mathbf{T}}\mathbf{Y} \tag{4-5}$$

$\hat{\mathbf{H}} = [\hat{b}_m \quad \hat{b}_{m-1} \quad \dots \quad \hat{b}_0 \quad \hat{a}_{n-1} \quad \hat{a}_{n-2} \quad \dots \hat{a}_0]^T$

Formulating $\mathbf{x_k}$ according to Eq. (4-6)

$\mathbf{X}=[\text{Real}(\mathbf{x}_1)\text{Imag}(\mathbf{x}_1)\dots\text{Real}(\mathbf{x}_n)\text{Imag}(\mathbf{x}_n)]^T$

$Y=[\text{Real}(y_1)\text{Imag}(y_1)\dots\text{Real}(y_n)\text{Imag}(y_n)]^T$

$yk=G_m(j?_k)(j?_k)^n \qquad k=1,2\dots N$

2. Re-formulate y_k by

$$y_k = \frac{G_m(jw_k)(jw_k)^n}{\hat{b}_m(jw)^m + \hat{b}_{m-1}(jw)^{m-1} + \dots + \hat{b}_1(jw) + \hat{b}_0}, k=1,2\dots N$$

Re-formulate x_k according to Eq. (4-7). Construct X and Y as step 1. Re-calculate the parameter vector $\hat{\mathbf{H}}$ using Eq. (4-5).

3. If the frequency response of $\hat{\mathbf{H}}$ fits the measurement, the procedure is completed. Otherwise, go back to step 2

$x_k = [(j?_k)^m (j?_k)^{m-1}\dots(j?_k)^1 \quad 1 \quad G_m(j?_k)(j?_k)^{n-1} \quad G_m(j?_k)(j?_k)^{n-2} \dots G_m(j?_k)]$ (4-6)

$$xk = \frac{[(jw_k)^m \ (jw_k)^{m-1} \ldots (jw_k)^1 \ 1 \ G_m(jw_k)(jw_k)^{n-1} \ G_m(jw_k)(jw_k)^{n-2} \ \ldots G_m(jw_k)]}{\hat{b}_m(jw)^m + \hat{b}_{m-1}(jw)^{m-1} + \ldots + \hat{b}_1(jw) + \hat{b}_0} \quad (4\text{-}7)$$

In the identifying process, MATLAB software is used in calculating the coefficients of numerator and denominator polynomials in transfer function respectively by LSE method.

4.1.2 Identification Results

The identification results are shown in Fig. 4-1, where the dashed line represents the measured frequency response and the solid line represents the frequency response from the estimated model. The transfer function of micro-mirror is shown in Eq. (4-8), whose poles and zeros are shown in Fig. 4-2.

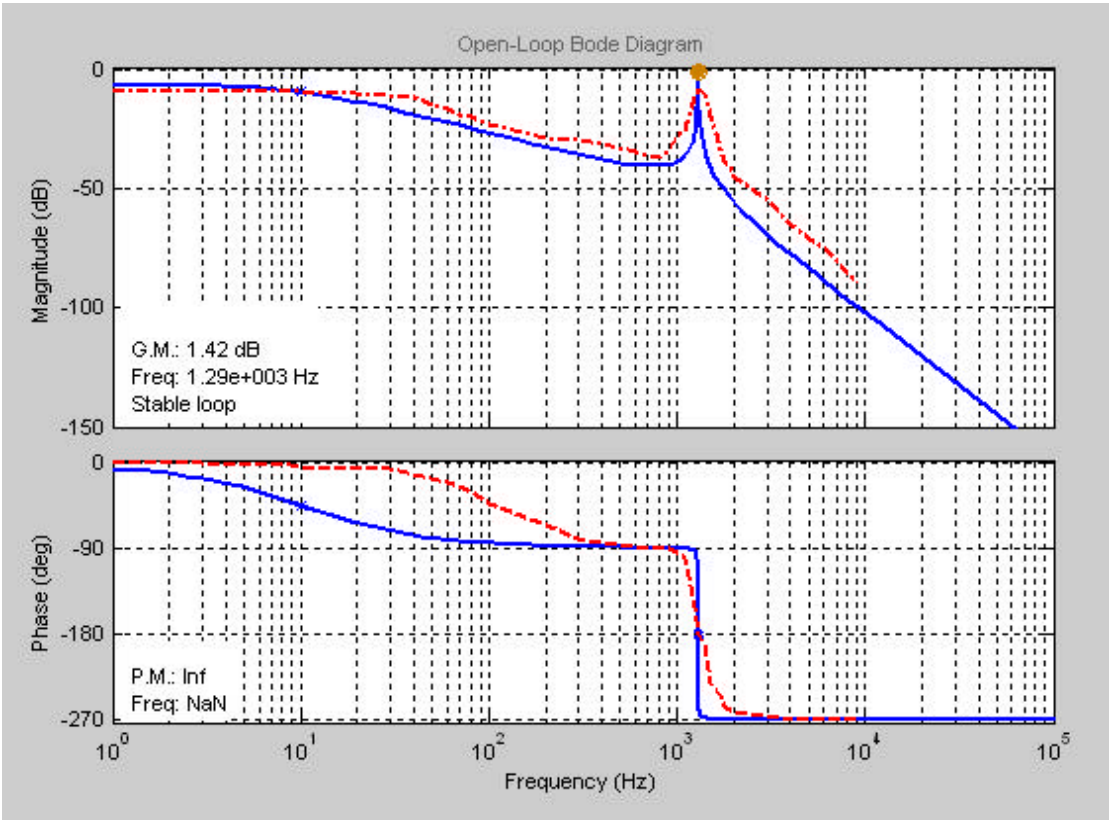

Fig. 4-1 The Bode plot of micro-mirror identified

Transfer function of MEMS mirror identified in frequency domain:

$$\frac{1.912*10^{9}}{s^{3}+97.09s^{2}+6.571*10^{7}} \qquad (4\text{-}8)$$

[Poles: (-0.0171 ± 8.1062i)*10^3,-0.0628*10^3]

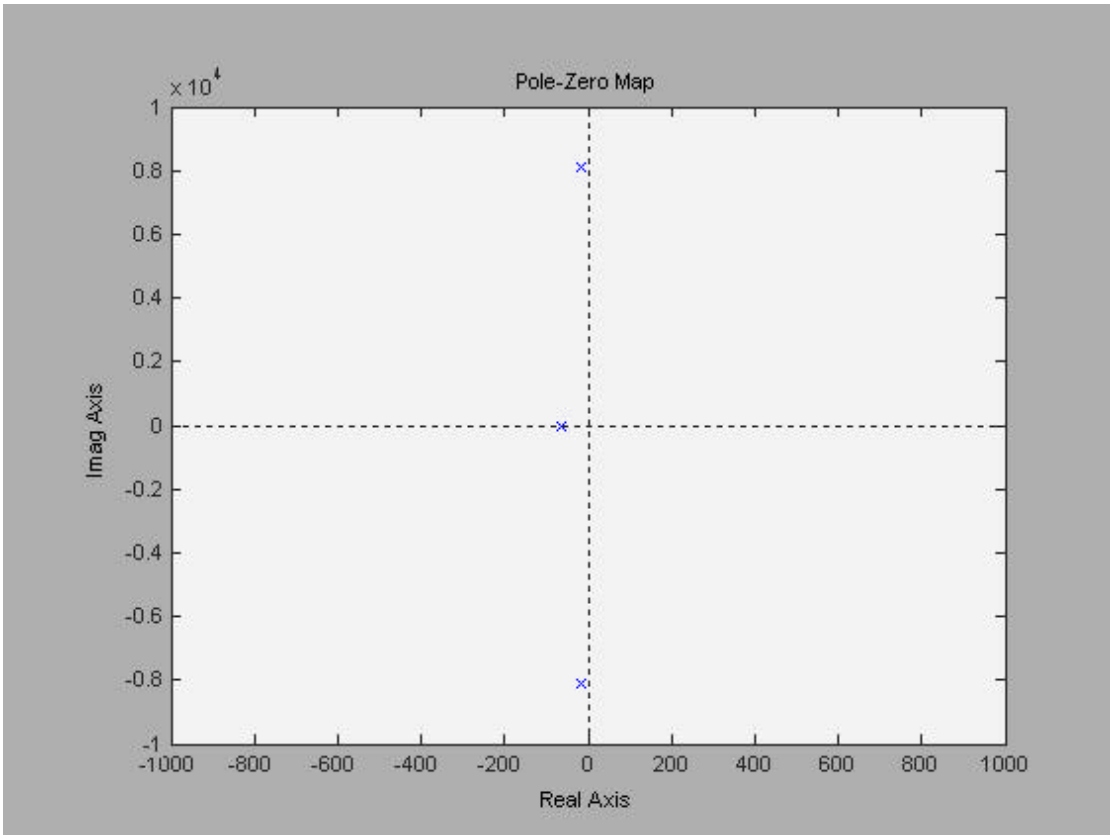

Fig. 4-2 Poles and zeros of identified model

In order to simplify the design process of compensator for tracking system, the transfer function of micro-mirror was usually reduced from three levels to two levels. According to identified model of micro-mirror, the real pole results in the low-frequency decay but the complex poles result in the high-frequency damping and overshoot. Since the micro-mirror is driven in high-frequency over 1 kHz, the low-frequency gain decay due to real pole can be neglected. The influences of

complex poles in micro-mirror are consequently emphasized to manifest the major characteristics of system. The compensators of tracking system were designed according to these major features of micro-mirror. The reduced transfer function of micro mirror was shown in Eq.(4-9). The reduced frequency response of micro-mirror was shown in Fig. 4-3.

Transfer function of MEMS mirror reduced to two levels:

$$\frac{3.04*10^7}{s^2+34.2s+6.571*10^7} \qquad (4\text{-}9)$$

[Poles: (-0.0171 ± 8.1062i)*10^3]

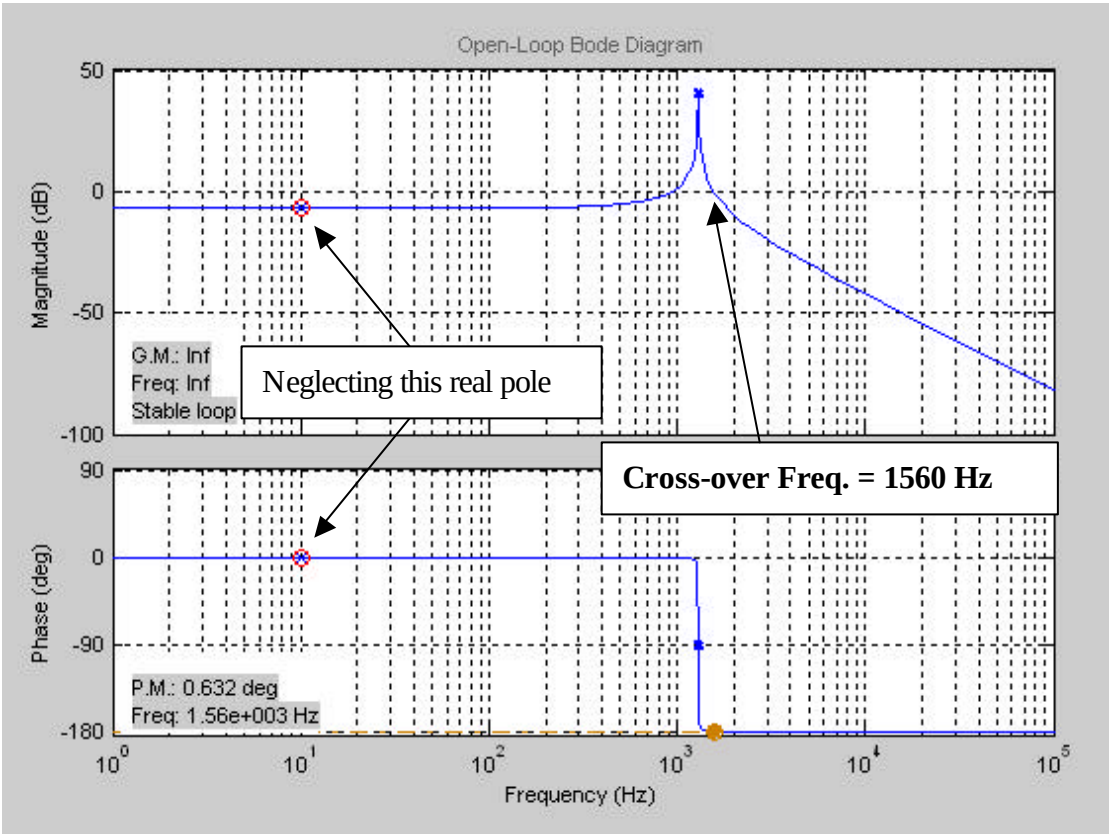

Fig. 4-3 The Bode plot of micro-mirror re-identified

4.2 Tracking system [25]

According to the identified model of MEMS mirror, many characteristics of

mirror can be found consequently to determine its performance. The tracking system uses mirror to follow the disk runouts and requires some compensators to improve its stability and error characteristics. By analyzing mirror's characteristics from the identified model, appropriate compensators can be designed to enhance system's performance.

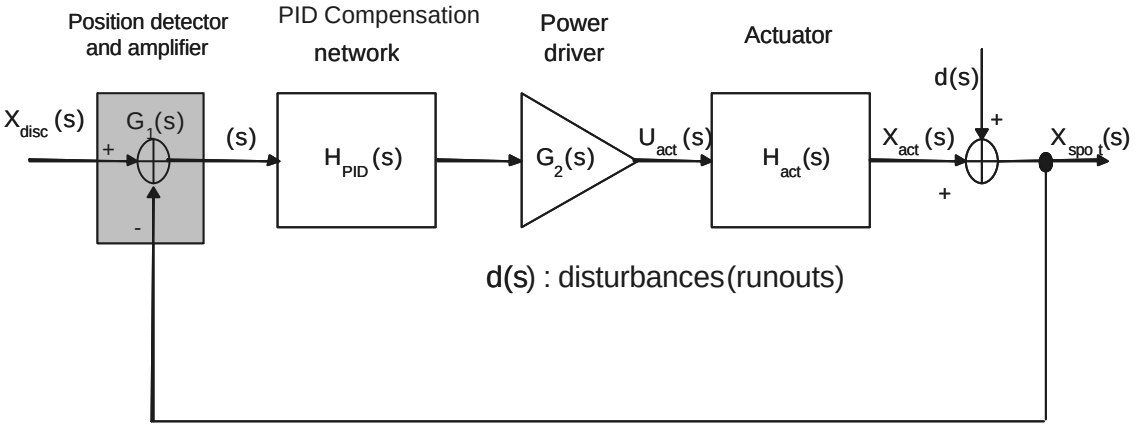

Fig. 4-4 The diagram of tracking control system

As shown in Fig. 4-4, the micro-mirror H_{act} is used as a tracking actuator to control the spot motion X_{act} in the radial direction on the optical disk. The d(s) is disturbances resulting from disk runout. The tracking error signal $G_1(s)$ based on push-pull method from the split detector is input to the PID compensator H_{PID} and the control signals were amplified by power driver $G_2(s)$ to control the micro-mirror.

4.2.1 Compensator design

Before designing the compensators, there are three requirements noted for designing a controller to compensate the tracking system.

1: Enhancement of system's bandwidth.

As described in Section 2.3, the objective lens mounted on a small actuator (usually a voice coil motor, VCM) must be controlled to follow the disk runouts (Focusing/Tracking) in real time. The frequency responses of these feedback systems (also referred to as servo system) have the bandwidth of several kHz. Now micro-mirror with higher first resonance 1.7 kHz than other actuators (VCM) 30 Hz compared in Figs. 4-5(a) and 4-5(b) was compensated more easily to extend the tracking system's bandwidth. The compensator was designed to enhance system's bandwidth further.

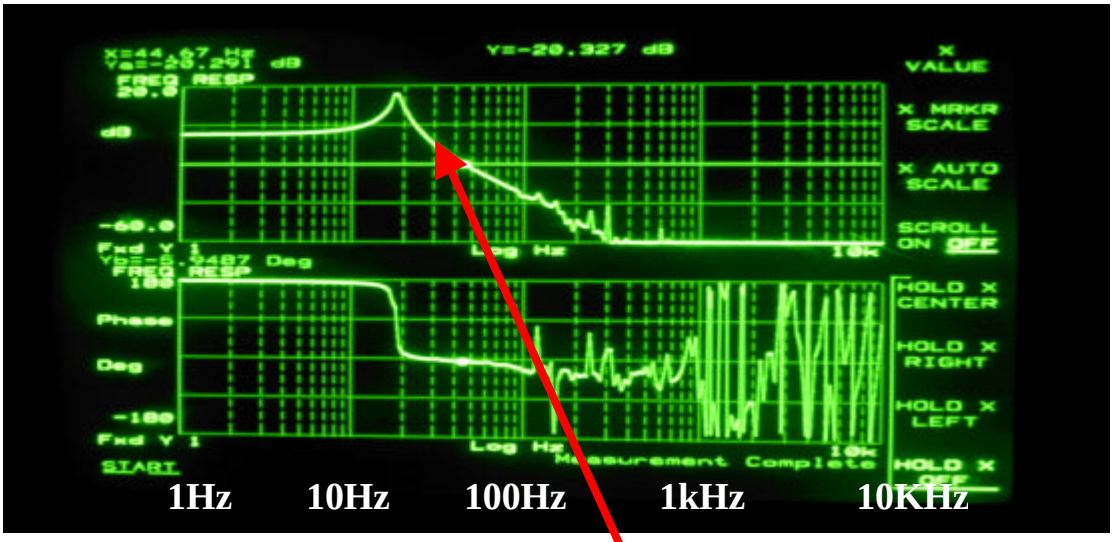

(a)VCM

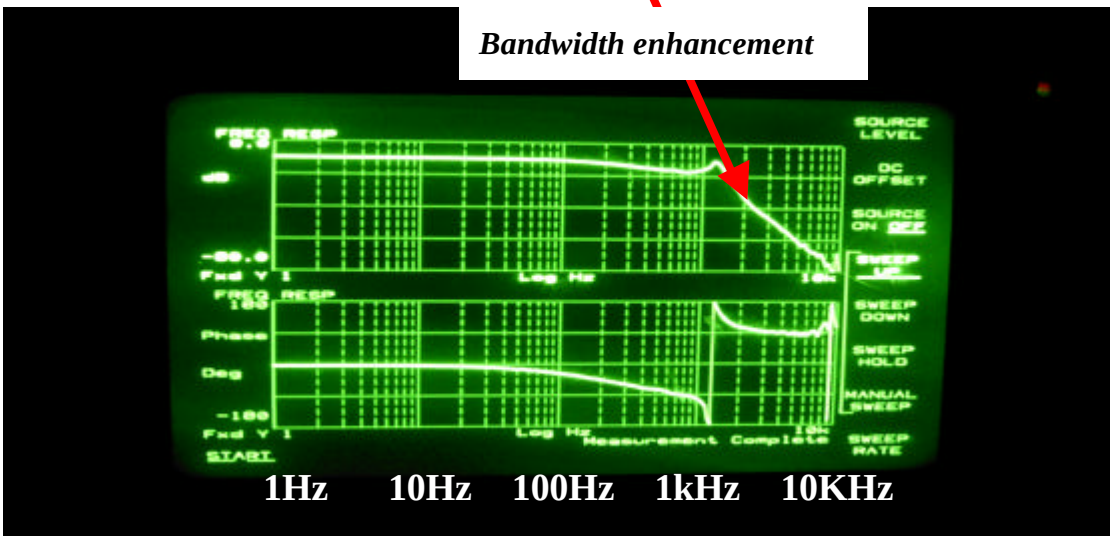

(b) MEMS mirror

Fig. 4-5 Measured frequency response of (a) voice coil motor (VCM) alone and (b) MEMS mirror alone

2: Enhancement of Low Frequency Gain

The runouts of optical disks are two to three orders of magnitude higher than the allowable focusing/tracking errors. Therefore, the laser spot driven by the actuator become hard to follow the disk runouts in the tracking process. Since the disk runouts are low frequency movements, the loop gain of tracking system in low frequency must be high enough to reduce the influences of runouts. In the design of tracking system, the loop gain needs to be enhanced by the compensator.

3: Improvement of Stability

In the design of a servo system, the stability of closed loop is a fundamental requirement. It is well known, a real system whose open loop frequency response approaches unity gain with -180 degrees phase lag has no margin of stability because even the slightest variation in system components could push the response into the unstable region. Therefore, it is common to use gain margin Gm and phase margin Pm as measurements of relative stability based on how close the open loop frequency response is to this unity gain, and -180 degrees phase point. Note that as |Gm| < 1 and negative Pm indicate an unstable system. For the design of tracking system, the gain margin and phase margin must be increased with compensator to improve the stability.

Gm (gain margin) = $\frac{1}{|GH(jw)|}$ where $\angle GH(jw) = -180$ degrees

Pm (phase margin) = 180 - $\angle GH(jw)$ where $|GH(jw)| = 1$

For the MEMS mirror the Gm and Pm can directly be read from the bode-plot in Figs. 4-1 and 4-3.

Gm=1.42 dB Pm= infinity (three levels)

Gm= infinity Pm= 0.632 (two levels)

Although the MEMS mirror is a stable system due to the positive Gm and Pm, it still requires a compensator to increase gain margin Gm and phase margin Pm for improving stability and eliminating the interferences of runouts.

4.2.2 Tuning of PID Controller [26]

For problems that need margin improvement and low-frequency gain improvement, it is effective to use both lead and lag compensations. By combining the derivative and integral feedback, the PID controller is obtained. Its transfer function is shown in Eq. (4-9).

$$D(s) = K(1 + T_D s + \frac{1}{T_I s}) = (K_P + K_D s + K_I \frac{1}{s}), \qquad (4\text{-}9)$$

where K is controller gain, T_D is the derivative time and T_I is the integral time. The compensating effects by PID controller are roughly equivalent to combine lead and lag compensators in the same design. Hence, it can provide simultaneous improvement in transient and steady-state responses.

The simulation of tracking system

The performance of two-level tracking system with or without compensators in open loop is discussed below. By using frequency-response methods such as, Root Locus and Bode plot, the design of feedback control system can be accomplished. From the simulation results, the optimal parameters of PID compensators were found. The Root Locus and Bode plot of open-loop tracking system without compensators are shown in Figs. 4-6 and 4-7. And the step response of tracking system without

compensators is shown in Fig 4-8.

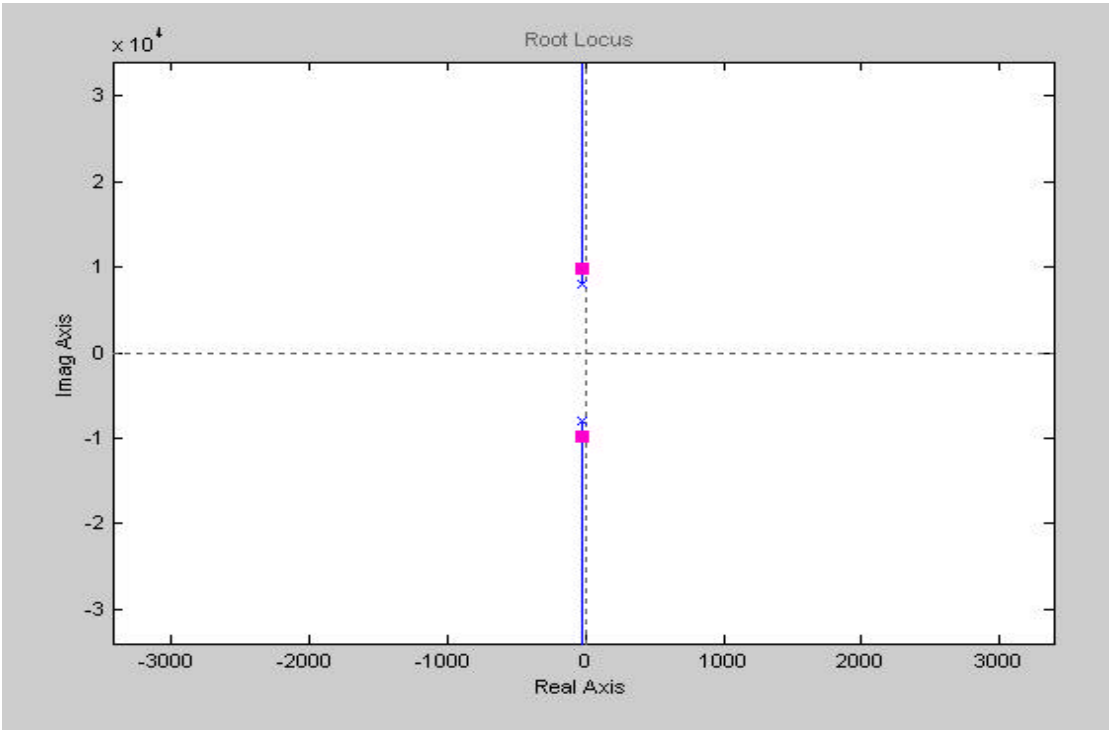

Fig. 4-6 The Root locus of tracking system without compensator

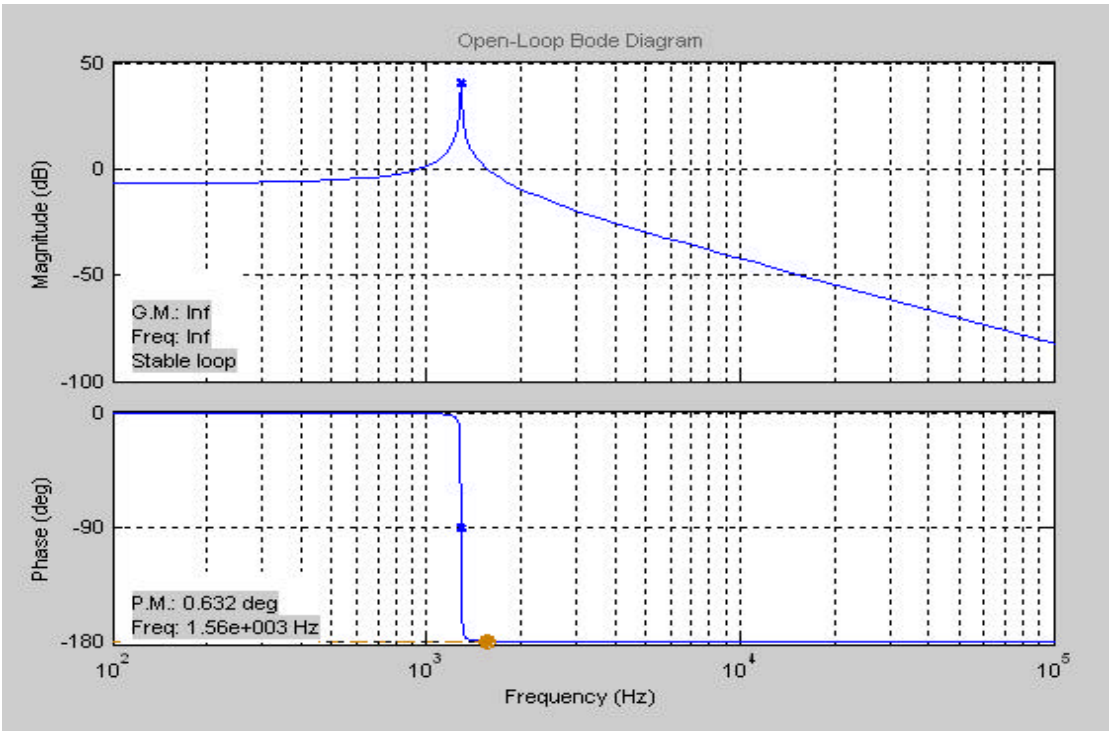

Fig. 4-7 The Bode plot of tracking system without compensator

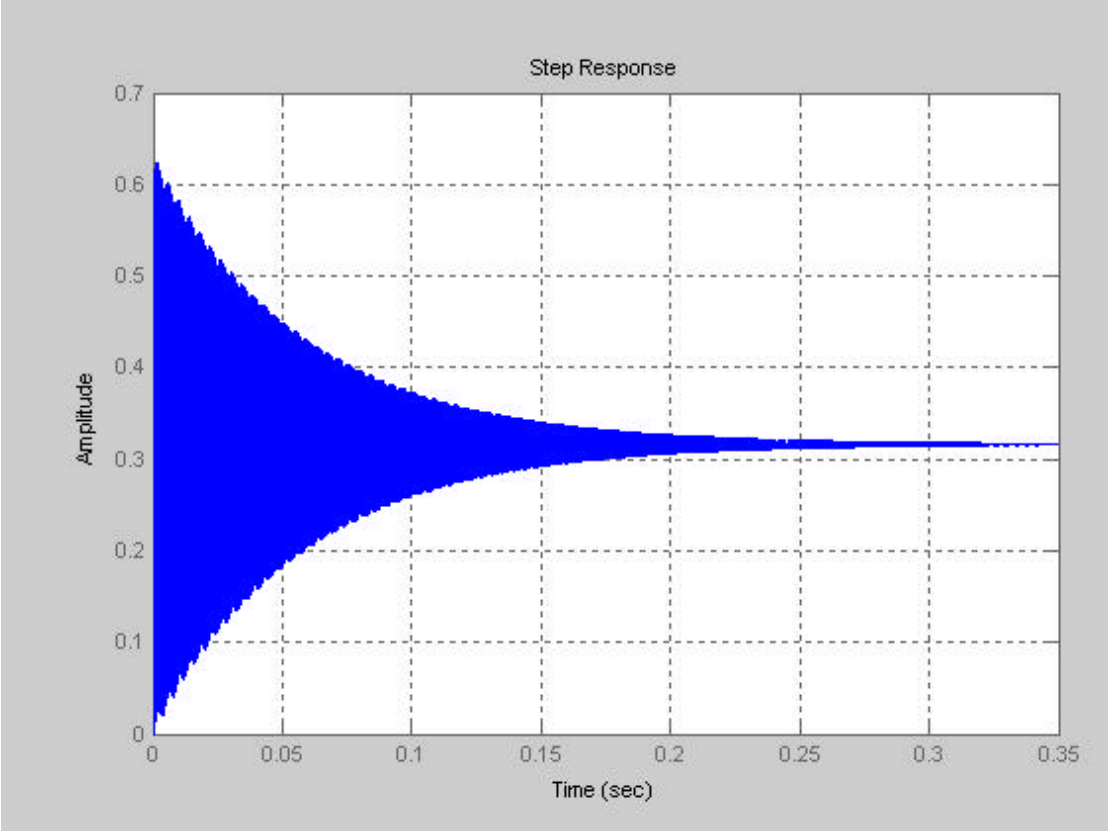

Fig. 4-8 The step response of tracking system without compensator

The poles in the left half plane in the Root Locus plot means that the tracking system is stable; the phase margin Pm of 0.62 degrees also means that the system was is in the stable state. From Fig. 4-8 the step response of system has serious damping and overshoot without compensators. A compensator is required to enhance tracking system's stability and loop gain.

By using MATLAB software, it can simulate if the closed –loop response for tracking system has already improved by compensators according to the knowledge of PID control. The PID controller has these tuning features that **proportional** feedback reduces errors, but high gains may destabilize the system, **integral** control improves the steady-state error and provides robustness with respect to parameter variations, but it also reduces stability and **derivative** control increases damping and improves stability. Based on this tuning rule, the optimal coefficients of

PID compensator in Eq. (4-9) were chosen to enhance bandwidth, loop gain and stability consequently. The Bode-plot of PID compensator is shown in Fig. 4-9. And the optimized tracking system with PID compensator is shown with better performance in Fig. 4-10, (Loot Locus), Fig. 4-11 (Bode-plot) and Fig. 4-12 (step response).

PID compensator transfer function:

$$C(s) = 20(S+8500)$$

Where $K_P = 170000$, $K_D = 20$, $K_I = 0$ comparing to Eq. (4-9)

Break-point f1=1353 Hz ($8500 = 2*\pi*f1$)

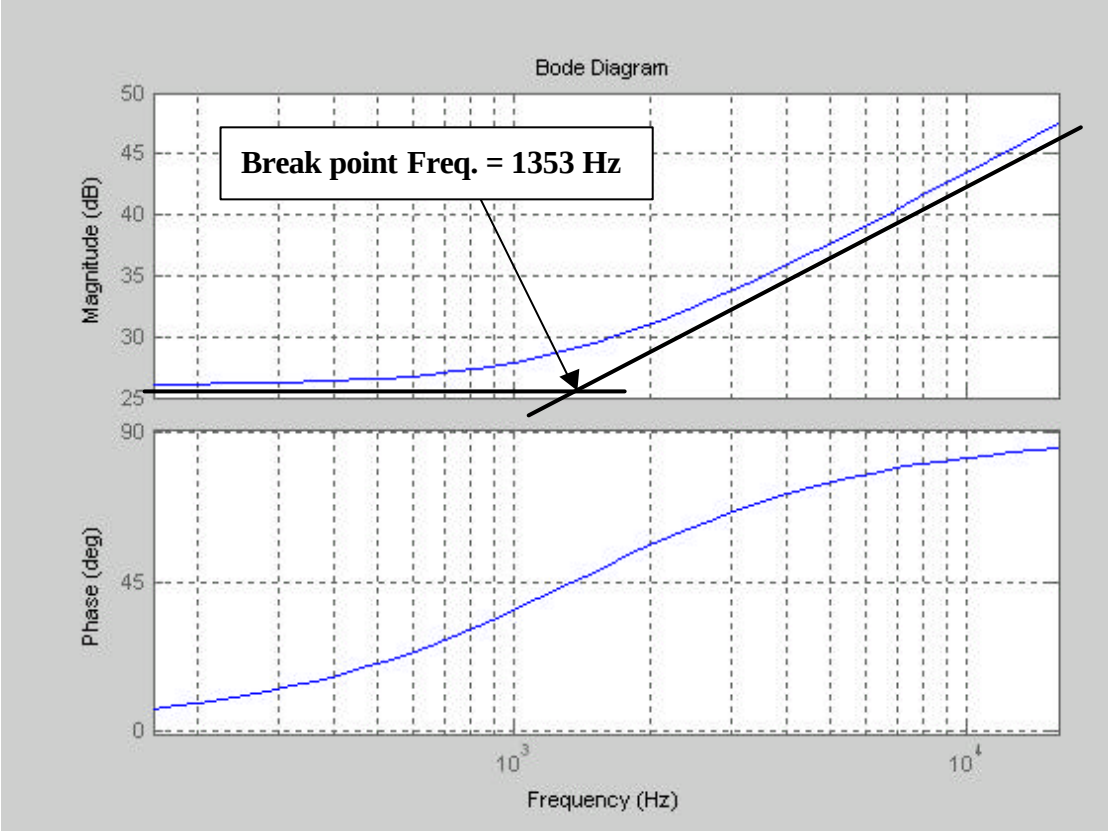

Fig. 4-9 The Bode-plot of PID compensator

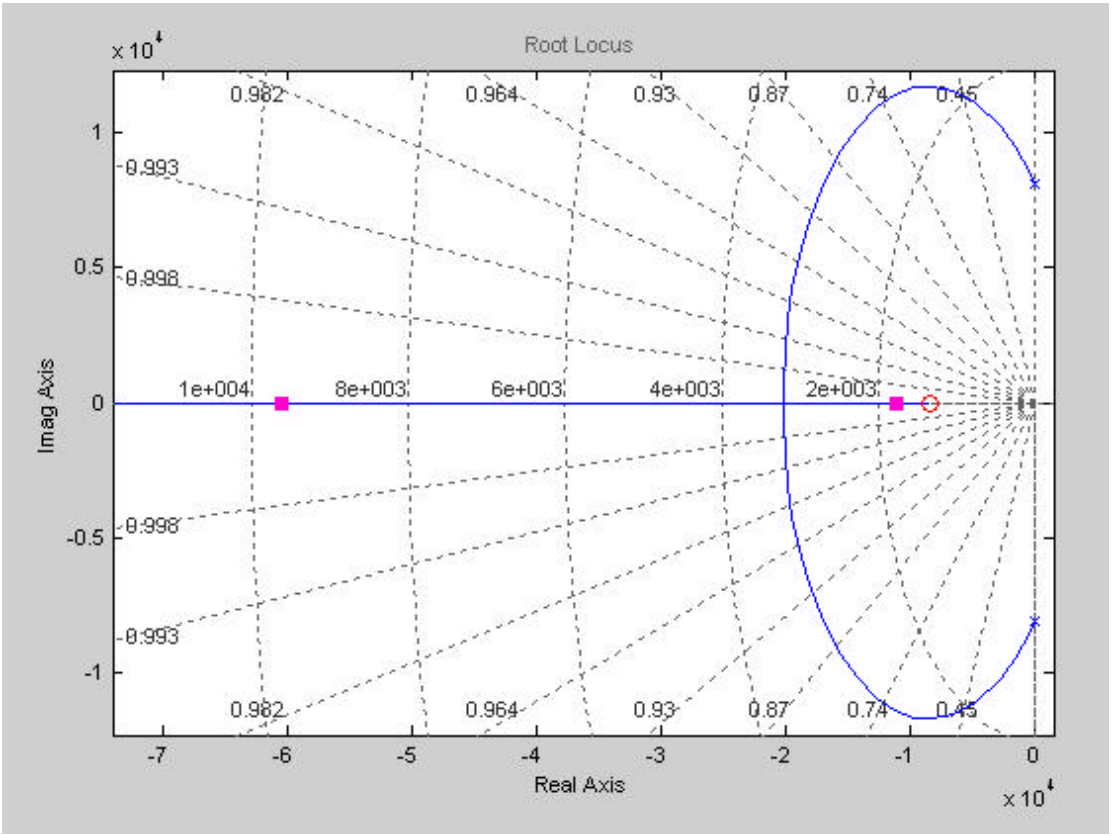

Fig. 4-10 The Root locus of tracking system with PID compensator

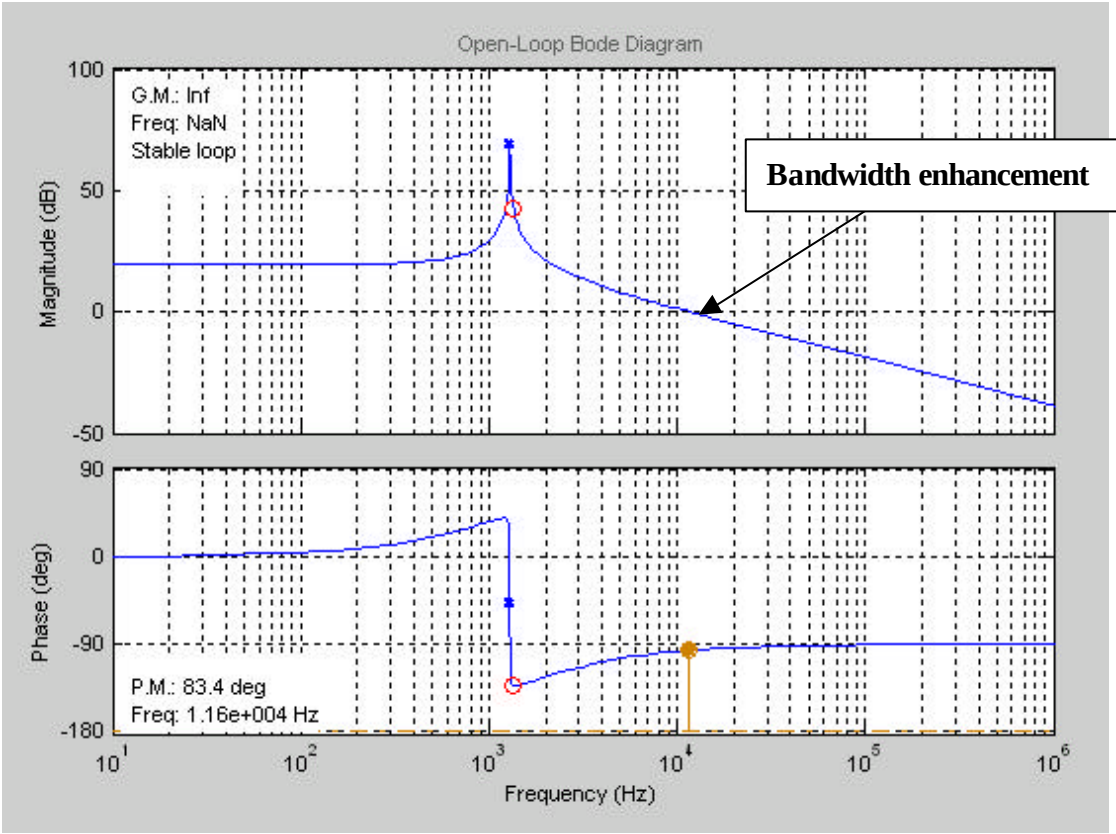

Fig. 4-11 The Bode-plot of tracking system with PID compensator

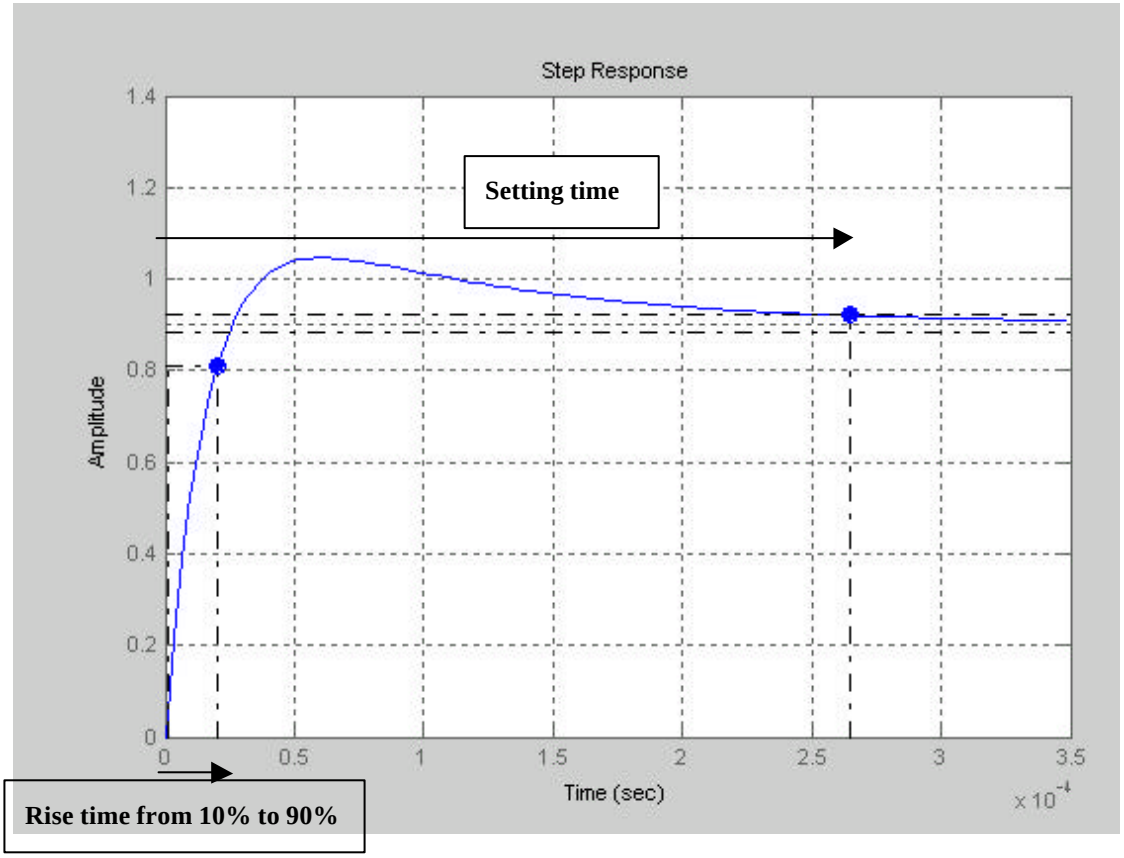

Fig. 4-12 The step response of tracking system with PID compensator

From the simulation results in Figs. 4-10, 4-11 and 4-12, we can find out that the tracking system is improved with the PD compensator. The micro-mirror is compensated to a more stable state by shifting the poles to the left in Root-locus plot. The phase margin Pm is enhanced from 0.62 degree to 83.4 degree. The loop gain in low frequency and the bandwidth (0dB point) of tracking system are also enhanced to 20 dB and 10 kHz by PD compensator. Consequently, the step response of the tracking system is quickly converged to steady-state, where had less overshoot and errors shown in Fig. 4-12. The rise time (from 10% to 90%) of tracking system is 20 us and the setting time (within 2%) is 0.26 ms.

4.3 Summary

Given the previous analysis of the simulation results, as well as the stated goal of extending the tracking system bandwidth and stability for an optimal system, the PID controller is determined according to the features of tracking system. The next chapter will look at the performance of the hardware prototype set to these optimal values determined from the simulation study.